INTERNATIONAL JOURNAL OF CLIMATOLOGY
Int. J. Climatol. **34**: 3913–3925 (2014)
Published online 18 February 2014 in Wiley Online Library
(wileyonlinelibrary.com) DOI: 10.1002/joc.3950

RMetS
Royal Meteorological Society

Review

Trends in precipitation extremes and return levels in the Hawaiian Islands under a changing climate

Ying Ruan Chen and Pao-Shin Chu*

Department of Meteorology, School of Ocean and Earth Science and Technology, University of Hawaii-Manoa, Honolulu, HI, USA

ABSTRACT: Trends of annual maximum 1-day precipitation in three major Hawaiian Islands are investigated using a nonparametric Mann-Kendall method and Sen's test (MKS). The records are from 24 stations on Oahu, Maui, and Hawaii, and the period of analysis ranges from 1960 to 2009. To complement the MKS method, a non-stationary three-parameter generalized extreme value (GEV) distribution is also used to detect trends in precipitation extremes. Both methods demonstrate that negative trends prevail for Oahu and Maui but positive trends dominate the Island of Hawaii. The influence of the location and the scale parameter in the GEV model on different return levels (2-year, 20-year, and 100-year) are explicitly described. The return-level threshold values are found to change with time considerably. As a result, a rare storm with daily precipitation of 300 mm (20-year return period) in 1960 has become a rather common storm event (3–5-year return period) in 2009 on the Island of Hawaii. The opposite trend behavior in extreme events is observed on Oahu and Maui, where rainfall extremes have become less frequent in the last five decades. A positive relationship is found between the precipitation extremes and Southern Oscillation Index (SOI), implying greater extreme events during La Niña years and the opposite for El Niño years.

KEY WORDS trends; changes in precipitation extremes and return periods; Hawaii

Received 21 March 2013; Revised 10 January 2014; Accepted 15 January 2014

1. Introduction

The changes in extreme events such as heavy precipitation and associated floods, heat waves, and hurricanes attract a lot of attention because of their devastating consequences on societies and their economies. Studies on changes in climate extremes using observations have been performed on both a global and regional scale. An increase in the number of warm summer nights, decrease in the annual number of frost days, and significant increase in the total wet day rainfall were noted by Frich *et al.* (2002), based upon global daily station observations. Alexander *et al.* (2006) also found a broad increase in precipitation indices globally. On a regional or continental scale, Groisman *et al.* (2004) identified significant positive trends in heavy and very heavy precipitation in the eastern part of contiguous United States. Griffiths and Bradley (2007) pointed out that in northeastern United States precipitation extremes are increasing. Recently, Chu *et al.* (2014) noted a prevailing upward trend in precipitation intensity (mm day^{-1}) and 5-day precipitation amounts during the typhoon season (July–October) over the last 60 years in Taiwan.

Located in the subtropical marine region, Hawaii is strongly influenced by the ocean climate, which provides adequate moisture and temperature variation. Annual temperature variation in Hawaii is small, about 5 °C (Giambelluca and Schroeder, 1998). The characteristics of precipitation, however, are highly spatially diverse due to the influence of complex topography with external forcings. The interaction of synoptic systems (e.g. upper tropospheric troughs, cold fronts, Kona lows, and tropical cyclones) with local topography results in flood-leading heavy rainfall events in Hawaii that cause damage to properties, agriculture, and public facilities (Schroeder, 1977; Chu *et al.*, 1993; Kodama and Barnes, 1997; Lyman *et al.*, 2005; Chu *et al.*, 2009). Pollutants carried away by heavy stream flows are one of the major threats to near-shores marine ecosystems, especially coastal coral reefs. Accordingly, scientific understanding of the trends of extreme precipitation events is of particular importance in the inclusive perception of climate change in Hawaii and relevant to policy concerns.

The statistics of extremes has been one of the research focuses of meteorology and hydrology during the past decade. Katz *et al.* (2002) examined some of the most popular approaches to extreme statistics. Characteristics of extreme events such as maximum precipitation, river peak flow, and streamflow are described. Examples of the application of the Generalized Pareto distribution (GPD)

* Correspondence to: P.-S. Chu, Department of Meteorology, University of Hawaii, 2525 Correa Road, Honolulu, HI 96822, USA. E-mail: chu@hawaii.edu

and the generalized extreme value (GEV) distribution to those extreme events are given. Katz *et al.* (2002) also demonstrated the use of GPD and GEV to downscaling of extremes. The GEV distribution is based on the statistical theory of extremes (Coles, 2001). Kharin and Zwiers (2005) estimated the return values of annual temperature and precipitation extremes in transient climate change simulations using a non-stationary GEV distribution with time-dependent location, scale, and shape parameters by the maximum likelihood method. They found that changes in precipitation extremes are due to changes in both the location and scale parameters. García *et al.* (2007) also used a non-stationary GEV distribution with time-dependent parameters to analyze the trends in block-seasonal extreme rainfall over the Iberian Peninsula. They discussed the influence of changes in location and scale parameters to the return levels.

On the basis of a stationary GEV distribution, Chu *et al.* (2009) estimated return periods of heavy rainfall in Hawaii using annual maximum daily rainfall. Spatial patterns of heavy rainfall events are mapped for each island; however, there was no attempt to study trends in precipitation extremes and return levels. Subsequently, Chu *et al.* (2010) used a nonparametric Mann-Kendall method and Sen's test to investigate trends in precipitation extremes in Hawaii. The precipitation extremes are derived from five of the 27 climate change indices defined by the Climate Variability and Predictability (CLIVAR) program, a component of the World Climate Research Program under the World Meteorological Organization. These indices include, daily precipitation intensity, annual number of days with daily precipitation $\geq$25.4 mm, annual maximum consecutive 5-day precipitation, and annual maximum consecutive dry days. In Chu *et al.* (2010), parametric distributions are not used to represent precipitation variability

Our current study focuses on extreme events using a parametric, non-stationary GEV, which tacitly assumes that extreme events are changing with time as the climate changes. Instead of the climate change indices used in Chu *et al.* (2010), the current study applies extreme precipitation values directly. Moreover, the non-stationary GEV method is applied to investigate how the return level of extreme precipitation in Hawaii changes with time. Subsequently, the non-stationary GEV method is also performed to examine the relationship between precipitation extremes and the El Niño-Southern Oscillation (ENSO). The reminder of the paper is organized as follows: Sections 2 and 3 describe the dataset and methods used in this study, respectively; results are presented in Section 4; followed by a summary and conclusion in Section 5.

2. Data

The National Weather Service (NWS) cooperative stations provided the daily rainfall dataset (TD3200) used in this study. The station data can be obtained from the National Climatic Data Center (NCDC) web site. In Hawaii, the winter rainy season runs from November to April. To keep the wet season data intact, the water year is defined from July to June of the next year. The starting year of a water year is chosen to represent that year or season; e.g. 1960 means from July 1960 to June 1961.

A preliminary analysis of the TD3200 dataset reveals that there are 294 stations with daily rainfall records in the Hawaiian Islands. However, some gauges only have short records and many of them have incomplete rainfall records. Detection of trends in extreme rainfall events using the parametric GEV distributions needs complete records gathered over a long time period.

To fill in the missing records for a gauge, a simple analysis is performed. If one month is missing from a station's records we compare that station with nearby stations that have complete records, and check to see if unusually large values exist. If abnormal precipitation values do not exist during the missing period from the neighbouring stations, which is the case here, the original annual maximum daily value with a missing record is retained and the station is considered as 'complete'. For those stations with incomplete records, the percentage of missing observations is approximately 2–8% of the entire records. This rate of missing gaps is quite small based on a study by Zolina *et al.* (2005) who suggested that if there is more than 25% missing in the data set, the trend estimate in heavy precipitation indices from the incomplete series would differ from that in the complete series. To further test whether the results of this study may be influenced by missing observations, we selected a station (Naalehu, Station number 22) with the most missing data (7.8%) among all 24 gauges. Results of rainfall intensity at various return periods are essentially the same between the complete and incomplete series. By filling a small portion of missing observations, we obtained 24 cooperative stations with 'complete' records of daily precipitation data from 1960 to 2009 (50-years) for three of the four major Hawaiian Islands (Oahu, Maui, and the Island of Hawaii). Kauai has only two long-term complete stations. Because these two gauges are not representative for the entire island, Kauai is excluded from the analysis.

The location and elevation information of the stations are found in Table 1 and Figure 1. The majority of rain gauges on Oahu are concentrated in the southeastern part where population is dense (Stations 1–8). Seven of the eight Oahu stations are located in the south-facing leeward areas; the only gauge (Station 6) in windward Oahu is in the eastern area. For Maui (Stations 9–16), most stations are located in the central valley with two gauges on the east island. The stations are more evenly distributed on the Island of Hawaii and the eight stations (Stations 17–24) are roughly evenly spaced. Due to the limited availability of stations, caution should be exercised when using the results discussed in Section 4 to represent island-wide or statewide characteristics.

In this study, the annual maximum daily precipitation data are analyzed. Because only the largest value is

Table 1. Locations and elevations of the cooperative stations. Island is also shown.

Station ID	Station name	Latitude (°N)	Longitude (°W)	Elevation (m)	Island
1	Honolulu Observ	21.32	158.00	0.9	Oahu
2	Honolulu Intl AP	21.32	157.93	2.1	Oahu
3	Moanalua 770	21.35	157.88	11.3	Oahu
4	Punchbowl Crater 709	21.32	157.85	103.0	Oahu
5	Pauoa Flats 784	21.35	157.80	499.9	Oahu
6	Waimanalo Exp Farm	21.33	157.72	19.5	Oahu
7	Wilhelmina Rise 721	21.30	157.78	335.3	Oahu
8	Waialae Kahala 715	21.27	157.78	3.0	Oahu
9	Puunene 396	20.87	156.45	69.8	Maui
10	Kahului AP	20.90	156.43	15.5	Maui
11	Spreckelsville 400	20.90	156.42	27.4	Maui
12	Hamakuapoko 485	20.93	156.35	97.5	Maui
13	Keahua 410	20.87	156.38	146.3	Maui
14	Haleakala RS 338	20.77	156.25	2121.4	Maui
15	Kula Hospital 267	20.70	156.37	923.5	Maui
16	Kihei 311	20.80	156.45	48.8	Maui
17	Paauilo 221	20.05	155.37	243.8	Hawaii
18	Hilo Intl Ap	19.72	155.05	11.6	Hawaii
19	Waiakea SCD 88.2	19.67	155.13	320.0	Hawaii
20	Kulani Camp 79	19.60	155.30	1575.8	Hawaii
21	Hawaii Vol NP HQ 54	19.43	155.27	1210.4	Hawaii
22	Naalehu 14	19.07	155.60	243.8	Hawaii
23	Opihihale 2 24.1	19.27	155.88	414.5	Hawaii
24	Lanihau 68.2	19.67	155.97	466.3	Hawaii

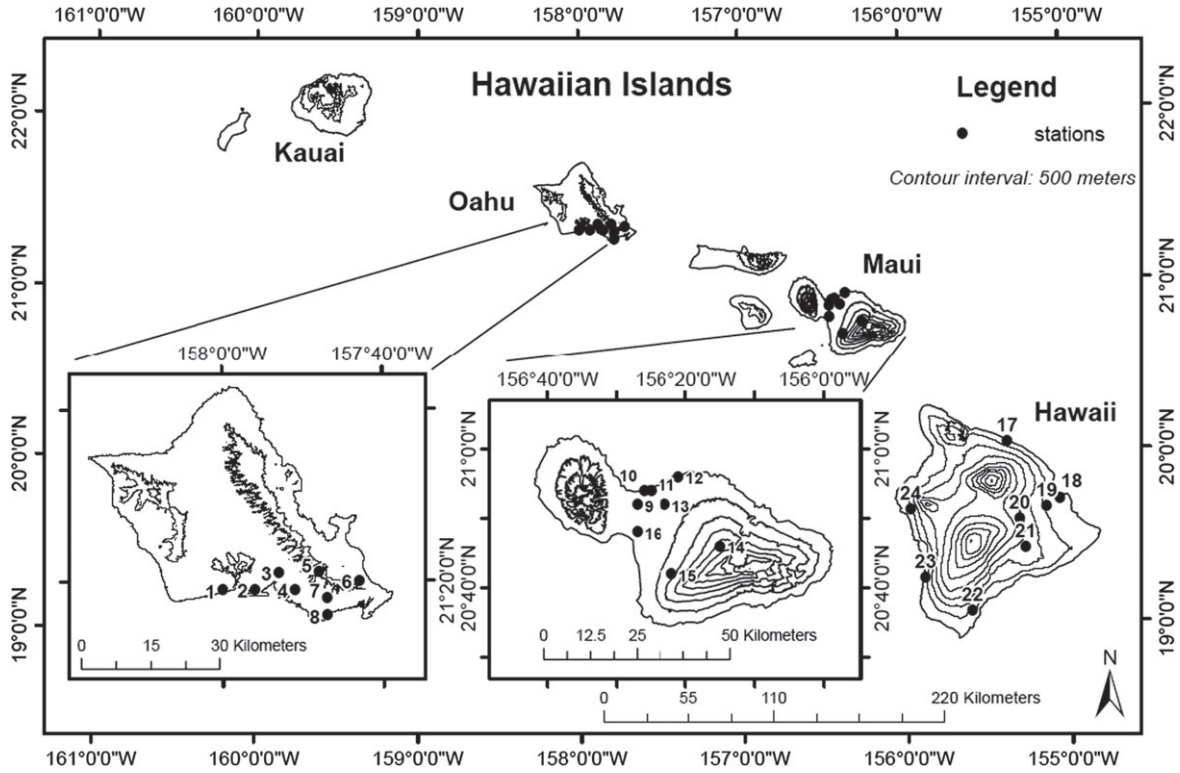

Figure 1. Location of the cooperative stations used in this study. The dark circles represent stations and the numbers are the station IDs, which correspond to those in Table 1.

chosen in each of n years, where n is the sample size, there is concern over whether this selection of the block maximum would cover the tail of an overall probability distribution of a precipitation series. For this purpose, histograms of daily precipitation and annual maximum daily precipitation series for two stations, one from Oahu and the other from the Island of Hawaii, are examined in Figure 2. Looking at the figure, it is clear that extreme precipitation data cover the right tail of the overall distribution rather well, justifying the use of the annual maximum daily precipitation to represent the underlying extreme-value statistics. To ensure stable

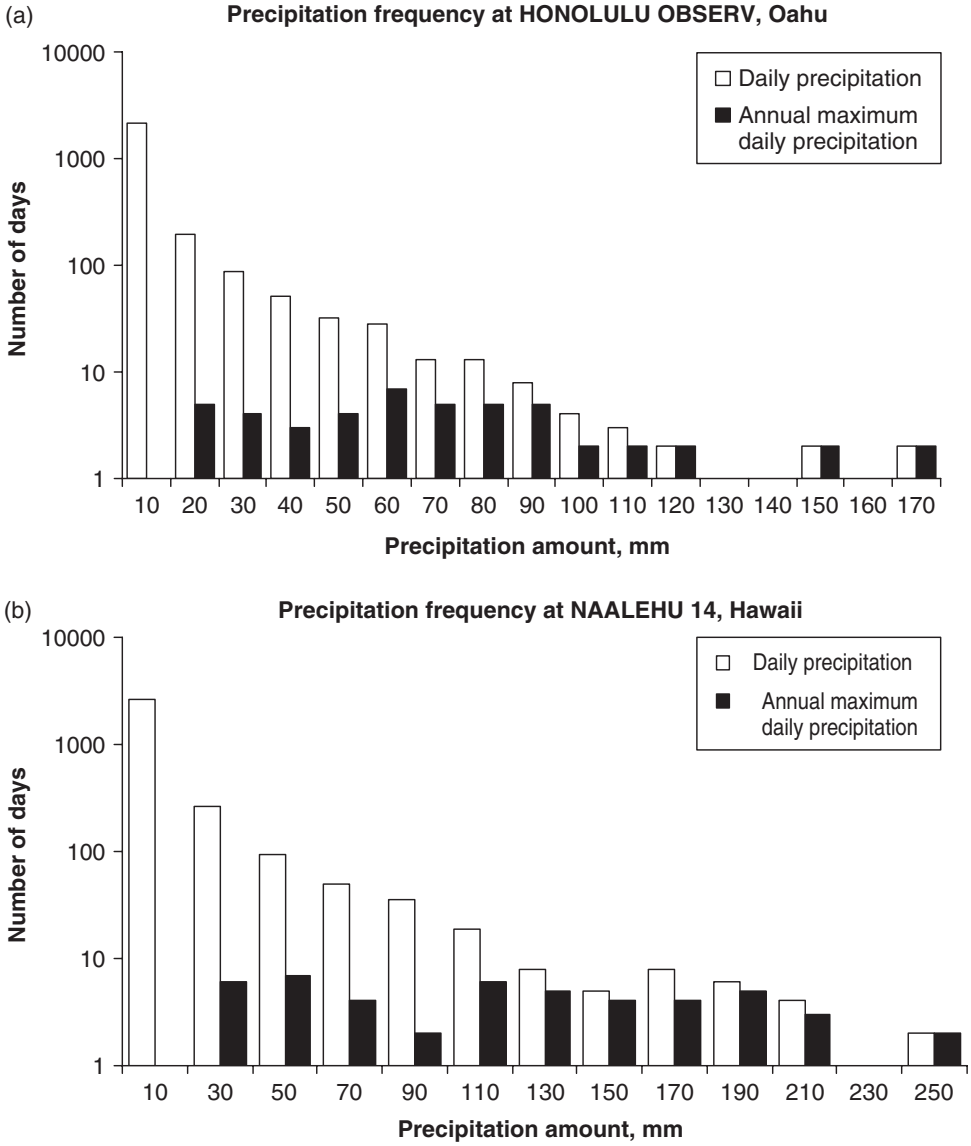

Figure 2. Histograms of precipitation frequency at (a) Honolulu Observatory, Oahu and (b) Naalehu Hawaii. Daily precipitation amounts are shown in unfilled bars and the annual maximum daily precipitation values are in filled bars.

results, the original data sets are first standardized before being analyzed. This transformation is also referred to as normalization. Centering and rescaling the original data (i.e. normalization) can improve the performance of the numerical optimization technique (Katz *et al.*, 2002). Note that the data sets will not follow a Gaussian distribution after this transformation unless the original ones do (Wilks, 2011).

Before performing trend-detection analysis, it is useful to test the records for possible inhomogeneities in the data such as abrupt shifts in the mean of the distribution (i.e. step-like changes in the mean of a time series). For this purpose, a nonparametric Mann–Whitney-Pettitt test (Pettitt, 1979) is used to examine possible inhomogeneities of the data sets. Results indicate that only two out of 24 stations show significant change points based on the annual maximum 1-day precipitation; therefore, the effect of inhomogeneities is small.

3. Methodology

3.1. Trend analysis

The methods used in this paper are discussed below. First, a nonparametric Mann-Kendall test and Sen's method (hereafter referred to as MKS) are applied to analyze whether the long-term trends are statistically significant (Mann, 1945; Kendall, 1970; Sen, 1968). The former allows the detection of monotonic patterns (e.g. linear, exponential) while the latter is basically a robust linear regression. The basic assumption of the Mann-Kendall test is that the data are independent. Because geophysical data are usually measured in a consecutive manner, temporal correlations are expected. When the test statistic is evaluated for its significance, if the persistence is strong the number of sample sizes that correspond to the degrees of freedom should be corrected (i.e. the effective sample size). A check of the autocorrelation functions of

precipitation extremes exhibits small values at various lags, reflecting a weak serial dependence in the block maximum precipitation data sets. As such, the data used can be considered as nearly independent. Subsequently, a non-stationary GEV distribution is fitted to detect whether there are time-dependent changes of the extremes.

3.2. A stationary GEV distribution

According to the description of the GEV theory (Coles, 2001; Wilks, 2011), for a large n the largest-of-n identically independent values follow a sample distribution with a cumulative distribution function given by

$$G(z) = \exp\left\{-\left[1+\xi\left(\frac{z-\mu}{\sigma}\right)\right]^{-1/\xi}\right\},$$
$$1+\xi\left(\frac{z-\mu}{\sigma}\right) > 0 \tag{1}$$

where μ, σ, and ξ are the location, scale, and shape parameter, respectively. The commonly used two-parameter extreme-value distribution such as the Gumbel distribution is a special case of the GEV where the GEV shape parameter approaches zero.

Estimates of the extreme quantiles, known as the return level z_p, corresponding to the return period

$$\tau = \frac{1}{p} \tag{2}$$

where p is the probability of occurrence, can be obtained by

$$z_p = \mu - \frac{\sigma}{\xi}\left[1-\{-\log(1-p)\}^{-\xi}\right], \quad \xi \neq 0. \tag{3}$$

As implied in Equation 3, the behavior of z_p depends on the location, scale, and shape parameters, and the return period τ (García *et al.*, 2007). Accordingly, both the location parameter μ and the scale parameter σ (because a negative sign appears in the second term on the right-hand-side of Equation 3) have a positive influence on the return level z_p. That is, the z_p in Equation 3, which is the return level corresponding to a return period τ, increases with increasing values of μ and σ. The shape parameter ξ has a negative impact on the return level z_p. For example, an increase in the value of ξ will result in a decrease in z_p, and this effect becomes more important when p in Equation 3 is smaller, which means a longer return period τ.

3.3. A non-stationary GEV distribution

Because this study is intended to analyze the time-dependent change in extreme precipitation, the GEV parameters mentioned previously are allowed to vary with time (t_0 stands for the initial time). Because the location and scale parameters play major roles in shaping the trend in precipitation extremes (e.g. Kharin and Zwiers, 2005; Garcia *et al.*, 2007) and the variability of the shape parameter is small (Hosking *et al.*, 1985), the assumptions of the parameters are

$$\mu_t = \mu_0 + \mu_1 (t - t_0),$$
$$\log \sigma_t = \sigma_0 + \sigma_1 (t - t_0), \xi \text{ is constant.} \tag{4}$$

The exponential expression (i.e. the inverse of exp is the logarithm function) for the scale parameter ensures a positive value for σ_t. For the shape parameter, it is kept constant in this study. Allowing the shape parameter to vary would likely cause numerical problems (R. Katz, personal communication). Also note that because both the location and scale parameters are expressed as a function of time, these parameters are not a fixed value and change with time. This is in contrast to the stationary GEV model described in Equation 1. If we substitute Equation 4 into Equation 3 the return level z_p becomes

$$z_p = \mu_0 + \mu_1 (t - t_0) - \frac{\exp[\sigma_0 + \sigma_1 (t - t_0)]}{\xi}$$
$$\times\left[1-\{-\log(1-p)\}^{-\xi}\right], \quad \xi \neq 0. \tag{5}$$

It is now obvious that the return level z_p is also a function of time. Therefore, the two non-stationary GEV model parameters and the associated return levels are not fixed in time, but are time dependent. Note that a stationary GEV model provides a fixed estimate of the return level for the entire time period. A non-stationary GEV, on the other hand, allows the return levels to change with time. This is perhaps more realistic in a changing climate.

Accordingly, a positive slope of the location parameter μ (i.e. $\mu_1 > 0$) will result in an increase in the return level, and vice versa. With a positive trend in the scale parameter (i.e. $\sigma_1 > 0$), the trend of return level z_p will increase as p decreases, or return period τ increases. The opposite is true for a negative trend in the scales parameter, (i.e. $\sigma_1 < 0$). This implies that the scale parameter σ has a special influence on return levels, which will be discussed later. The precipitation amounts for the 2-, 20-, and 100-year return periods, which correspond to probabilities 0.5, 0.05, and 0.01, are calculated for annual maximum 1-day precipitation.

The parameters of the non-stationary GEV distribution are estimated by the Extreme Toolkit using the R statistical programming language developed by University Corporation for Atmospheric Research (UCAR), which is available on the UCAR web page (http://www.isse.ucar.edu/extremevalues/evtk.html). The statistical significance of the parameters from a non-stationary model, where both location and shape parameters are time-dependent (M_1), can be assessed by the likelihood ratio test (Wilks, 2011) through comparison with a stationary model (M_2)

$$D = 2\{l(M_1) - l(M_2)\} \tag{6}$$

where $l(M_1)$ and $l(M_2)$ are the maximized log likelihood function of models M_1 and M_2, respectively. The statistic D is distributed according to a chi-square

distribution, with the degree-of-freedom parameter being the difference in the number of parameters between models M_1 and M_2. A large value for D indicates that M_1 explains more data variance than M_2; therefore M_1 is a better model than M_2.

3.4. A non-stationary GEV model with a covariate

In addition to estimating changes in extreme precipitation with time, non-stationary GEV can also be used to analyze whether the extreme precipitation is co-varying with another climate variable, such as the Southern Oscillation Index (SOI) which is commonly used to monitor the behavior of the El Niño and La Niña. In this case, t and t_0 in Equation 5 are replaced by time-variant SOI indicators (e.g. SOI(t) and SOI(t_0)). Thus, another set of time-variant location and scale parameters can be estimated to show the relationship between the precipitation extremes and SOI values.

3.5. Statistical field significance

For a given data set, it is reasonable to expect a certain number of stations or grids to pass a random local significance test. We assume that N out of the M stations ($N < M$) reach local significance at the 5% level from a trend analysis. At this test level, 5% of M stations might be significant by chance even if the true slope were zero. If the actual number of total stations showing local significance (N) exceeds that by random chance the spatial pattern may be considered 'field significant.' However, because of spatial correlation in geophysical data, the percentage of the field showing significant results should be far greater than that by chance. It is thus necessary to address the collective significance of a finite set of individual hypothesis tests for the entire field (Livezey and Chen, 1983).

The field significance of trend patterns is evaluated by Monte Carlo simulations (Chu and Wang, 1997; Douglas *et al.*, 2000). Time series of extreme precipitation series at each station for the period 1960–2009 are concurrently shuffled using a random number generator. Trends in GEV parameters and return levels are estimated at each station. The total number of stations showing significance at the 5% test level are counted and denoted as N_{mc}^{i}, where the superscript i denotes the ith trial and the subscript mc denotes the Monte Carlo experiment. This procedure is repeated for a large number of trials (5000 times) by resampling the original data. The field is considered to be significant at the 5% level when N exceeds N_{mc}^{*}, where N_{mc}^{*} is the 95th percentile of a locally significant trend from 5000 trials.

4. Results

4.1. Trends of 1-day maximum precipitation using a nonparametric Mann-Kendall and Sen's method

One of the major purposes of this research is to investigate whether the precipitation extremes in Hawaii have changed with time. Accordingly, we first estimated the trends of the 1-day precipitation amounts using the MKS method. Results are given in Table 2. Because we are interested in determining whether there are upward or downward trends and the significance of the trends, only the sign of the slope and their significance are provided.

Table 2. Signs of the slopes of Mann-Kendall and Sen's method (MKS) and non-stationary GEV parameters from 1960 to 2009. Stations 1–8 are on Oahu, 9–6 on Maui, and 17–24 on the Island of Hawaii.

Station ID	1-day maximum precipitation		
	MKS	GEV μ_1	GEV σ_1
1	−	−	−
2	−	−	+
3	− (*)	− (*)	− (*)
4	− (*)	−	−
5	− (*)	− (*)	− (*)
6	−	−	+
7	−	−	−
8	− (*)	− (*)	− (*)
9	−	−	−
10	−	−	−
11	−	−	−
12	−	− (*)	− (*)
13	−	+	−
14	−	−	−
15	−	−	−
16	−	−	−
17	+	+	−
18	+	+	+
19	+	+	+
20	+	+	+
21	+	+	+
22	+	+	+
23	+	+	+
24	+	+	+

+, positive trend; −, negative trend; *, 5% significant level.

As illustrated in Table 2, a high island-wide consistency in the sign of the slopes is noted (under MKS). The most dominant features are the negative trends for Oahu and Maui. That is, pronounced downward trends are displayed at all of the eight stations on Oahu (Stations 1–8) and eight stations on Maui (Stations 9–16). Specifically, trends at gauges 3, 4, 5, and 8 on Oahu show significance at the 5% level based on the MKS method. In projecting future precipitation changes for Oahu, Norton *et al.* (2011) used nonlinear neural networks to downscale daily extreme precipitation events from general circulation model outputs. They noted a prevailing downward trend in heavy precipitation intensity for the southern shoreline of Oahu during the next 30 years (2011–2040). Therefore, the projected decrease in storm precipitation intensity appears to be in line with the observed trend during the past 50 years.

Because the majority of gauges on Oahu are concentrated in the southeastern portion of the island where population is dense, there is concern over whether urbanization would affect trend results. For Oahu, there is a single gauge (Station 6) on the windward side where

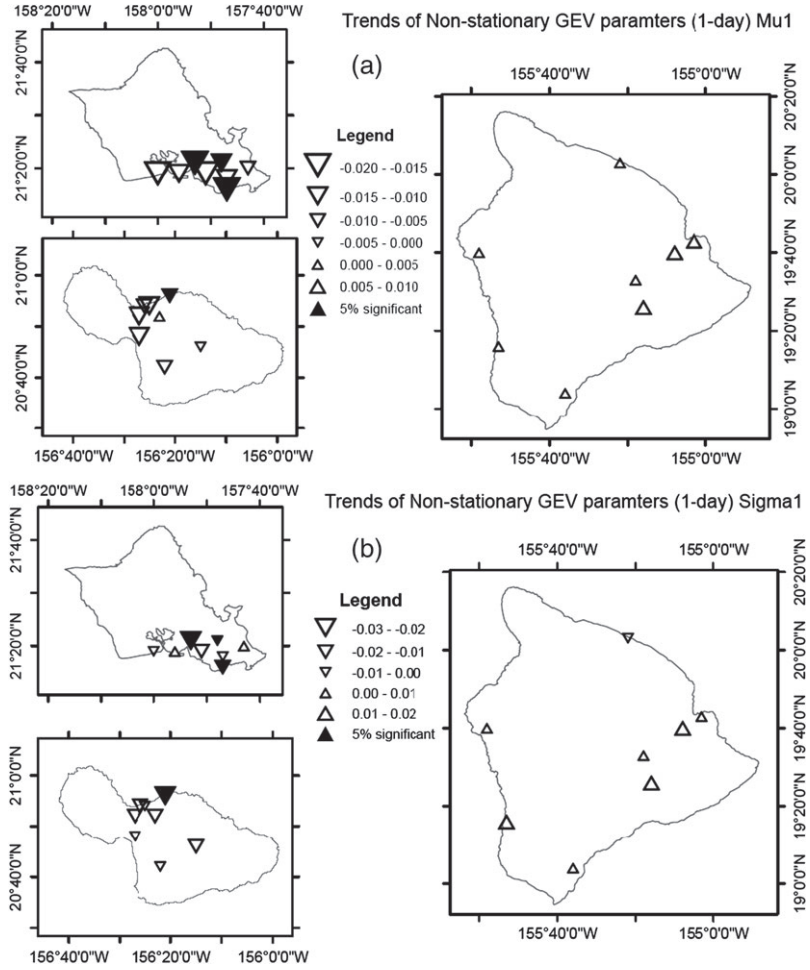

Figure 3. Spatial pattern of trends for (a) location parameter μ_1 and (b) scale parameter σ_1 for 1-day maximum precipitation according to non-stationary GEV distribution. Triangles denote the locations of the individual stations. Upward (downward) triangles indicate positive (negative) direction of change, and their size corresponds to the magnitude of trends. Black triangles indicate trends significant at the 5% level. Field significance is reached for Oahu in both (a) and (b).

population is less dense. This gauge also shows a downward trend in maximum precipitation since 1960, consistent with seven other leeward stations. Note that all eight stations on Maui, whose population is comparatively lower than Oahu, also display a downward trend. This includes even the high elevations gauges such as Haleakala (2121 m) and Kula Hospital (924 m) with very few inhabitants. Results from Maui and Oahu support the fact that the urbanization is not likely to cause an island-wide downward trend in precipitation extremes. In contrast to Oahu and Maui, positive trends prevail on the Island of Hawaii (Stations 17–24) although none of them are significant. In summary, since 1960 precipitation extremes follow a downward trend on Oahu and Maui and positive trends for the Island of Hawaii.

4.2. Trends of 1-day maximum rainfall using a non-stationary GEV distribution

4.2.1. Trends of the non-stationary GEV parameters

Apart from the statistical results from the aforementioned nonparametric method, the trends of two non-stationary GEV parameters (i.e. μ_1 and σ_1 in Equation 5) are given in Table 2. The stars in Table 2 indicate that the fit of the non-stationary GEV is significantly better than its stationary counterpart through Equation 6.

Spatial patterns of the trends of the two parameters of 1-day maximum precipitation are provided in Figure 3. There are prevailing negative trends on Oahu and Maui but positive trends on the Island of Hawaii for the location parameter μ_1 (Figure 3(a)). These highly resemble the trends of the extremes based on the MKS method (i.e. Table 2). According to the likelihood ratio test, the non-stationary GEV is significant at the 5% level at Stations 3, 5, 8, and 12 (Figure 3(a)). The trends of the scale parameter σ_1 are not always in the same direction as those of location parameter μ_1 (Figure 3(a) and (b)), and their effect will be discussed later. Results also show that the negative trends on Oahu in Figure 3(a) and (b) are field significant.

4.2.2. Trends of the return levels

After calculating the parameters of a non-stationary GEV distribution, the return levels (z_p) corresponding to different return periods can be estimated according

to Equation 5. The trends of the return levels are also determined using the MKS method.

Before looking at the details of the spatial patterns of the trends of return levels, it is instructive to understand the influence of the trends for location parameter μ and scale parameter σ. As shown in Equation 5, assuming the shape parameter ξ remains constant, the trend of a certain return level z_p is mainly determined by three components – the trend of the location parameter (μ_1), scale parameter (σ_1), and value of probability p, which is inversely related to return period τ via Equation 2. A positive trend for the location parameter μ (i.e. $\mu_1 > 0$) will inherently induce a positive trend for the return level. For the third term on the right-hand-side of Equation 5, the effect is more complicated. As discussed in Section 3.3, when there is a positive trend of the scale parameter σ (i.e. $\sigma_1 > 0$), the return level tends to increase when p decreases, which means a greater return period τ (i.e. 20-year, 50-year, 100-year or longer). However, when the scale parameter shows a negative trend (i.e. $\sigma_1 < 0$), the return level tends to decrease when p decreases, which means a greater return period τ (i.e. 20-year, 50-year, 100-year, or others). That is to say, the trends of 2-, 20- and 100-year return levels are different from each other due to the influence of the scale parameter σ. When a positive (negative) trend in the location parameter μ (i.e. positive trend of 2-year return level at a station) is embedded with a positive (negative) trend of scale parameter σ, then the trends of 20- and 100-year return level will be steeper than that of the 2-year return level. On the other hand, when the trend of the scale parameter σ acts to counteract that of the location parameter μ, the slope of the 20- and 100-year return level tends to become gentler than that of the 2-year return level or the sign may change.

To further explain the complex relationships among these three components in shaping the direction of trends, we look at the return levels at three stations as examples. Figure 4 shows the time series of return levels of 1-day maximum precipitation at Moanalua, Hawaii Volcanoes National Park , and Paauilo, which are Stations 3, 21, and 17, respectively (Table 1). Note that results presented in Figure 4 are obtained after transforming the standardized data back to the original space. This is accomplished by multiplying the standard deviation to the transformed data and then adding back the mean value at each station. It also should be noted that the variance of 1-day precipitation extremes is not constant for Moanalua, Oahu and Hawaii Volcano National Park, Hawaii (Figure 4(a) and (b)); it decreases or increases with time. This implies a non-stationary feature in the data. For Paauilo, Hawaii (Figure 4(c)), the series is characterized by quasi-periodic cycles mixed with a long-term decrease in precipitation extremes. Other stations also exhibit behavior suggestive of nonstationarity, justifying the use of the non-stationary GEV model to describe the data.

According to results presented in Table 2, the first station in Figure 4 has negative trends in both the location parameter μ_1 and the scale parameter σ_1. This

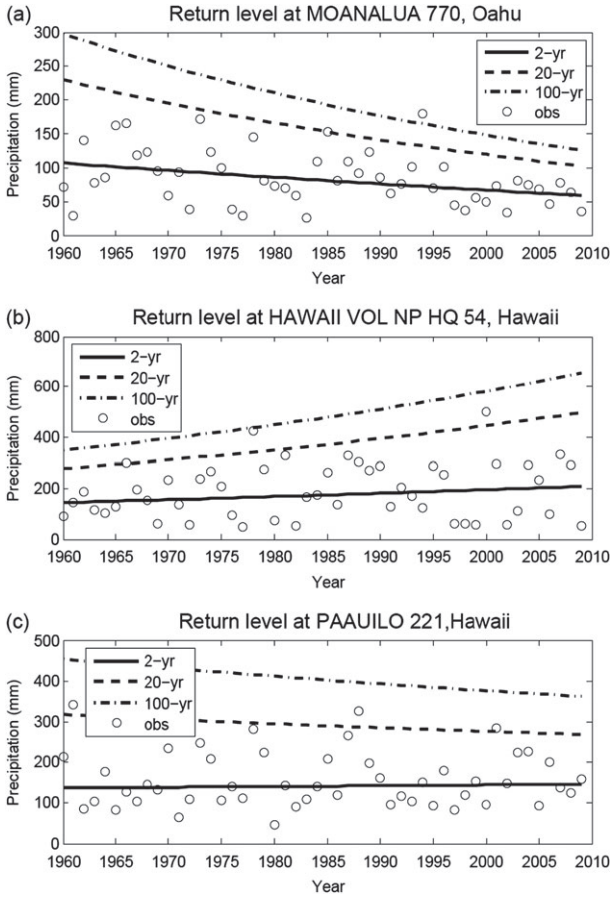

Figure 4. Time series of return levels for 1-day maximum precipitation at (a) Moanalua, Oahu, (b) Hawaii Volcanoes National Park HQ 54, Hawaii, and (c) Paauilo, Hawaii according to non-stationary GEV. The solid, dashed, and dash-dot lines represent the 2-year, 20-year, and 100-year return levels, respectively. The circles stand for observation data.

combination leads to decreasing trends in the three return levels, and the negative trend associated with 20- and 100-year return levels drops more dramatically than that of the 2-year return level (Figure 4(a)). Specifically, the quantiles corresponding to 2, 20, and 100 years return periods dropped from 107 mm in 1960 to 59 mm in 2009, from 230 mm in 1960 to 102 mm in 2009, and from 298 mm in 1960 to 126 mm in 2009, respectively. On the other hand, for Hawaii Volcanoes National Park, there are positive trends in both the location parameter μ_1 and the scale parameter σ_1 (Table 2). As a result, the three return levels all increase, and 20- and 100-year return levels increase more considerably (Figure 4(b)). For instance, an event with a 20-year recurrence interval in 1960 is about 300 mm. By 2009, it is about 420 mm; alternatively, an event with a 20-year recurrence-interval threshold values in 1960 has occurred on average once every 3 to 4 years by 2009. For Paauilo, however, a positive trend is found in the location parameter (μ_1) and negative trend in the scale parameter (σ_1) (Station 17 in Table 2). Due to the combination of these opposite signs, the 2-year return level increases slightly, while both 20- and 100-year return levels decrease more significantly (Figure 4(c)).

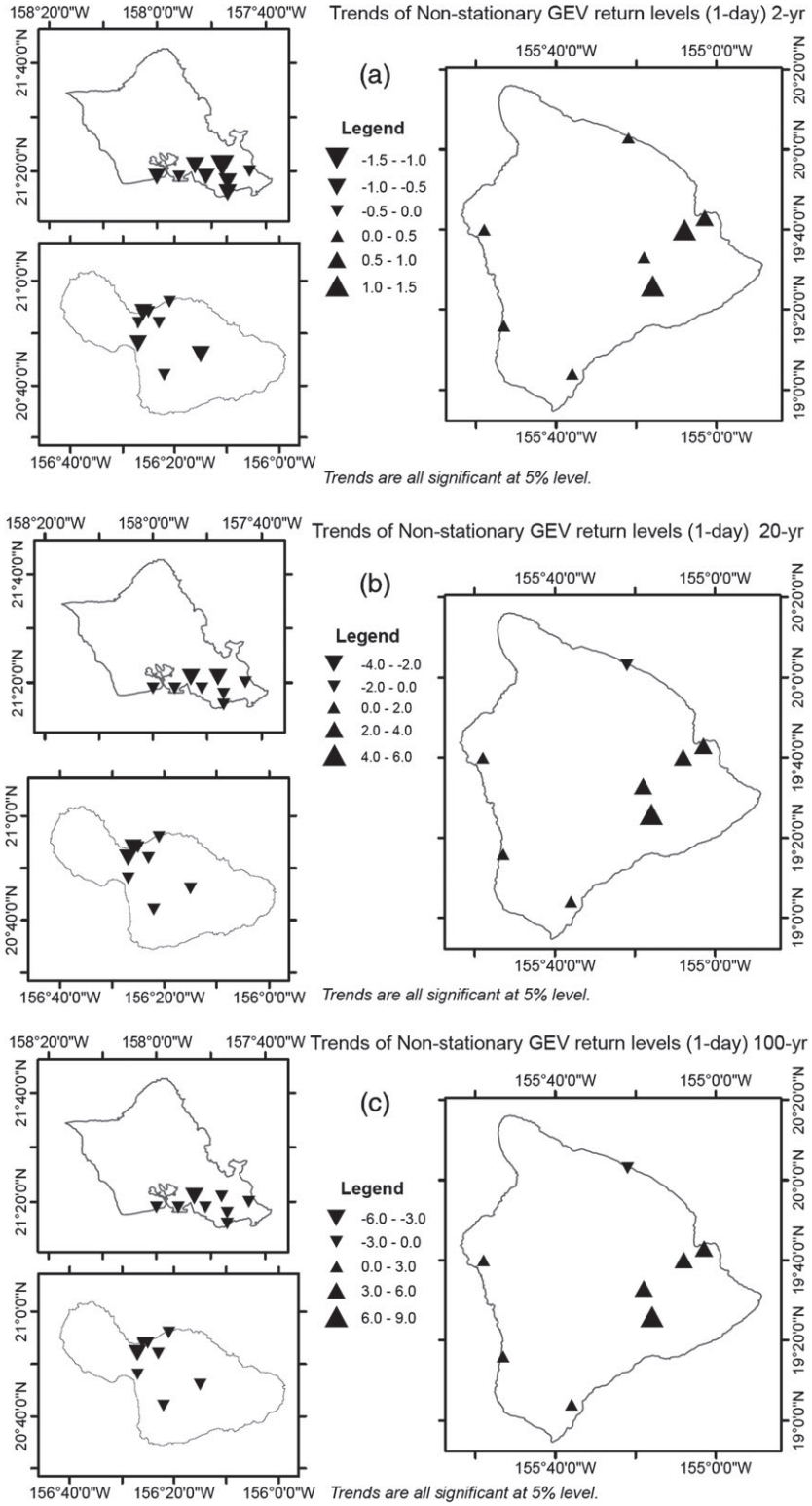

Figure 5. Spatial pattern of trends for non-stationary GEV return level for 1-day maximum precipitation, (a) 2-year, (b) 20-year, and (c) 100-year. Triangles denote the locations of individual stations. Upward (downward) triangles indicate positive (negative) direction of change, and their size corresponds to the magnitude of trends. All the trends are significant at 5% level. Field significance is reached in (a), (b), and (c).

The spatial patterns of the trends in the three return levels of 1-day maximum precipitation are given in Figure 5. The three return levels are for return periods 2-year, 20-year, and 100-year and they correspond to probabilities 0.5, 0.05, and 0.01, respectively. The most salient feature of the three return levels is the prevailing negative trends on Oahu and Maui and positive trends on the Island of Hawaii. Field significance is reached for all panels in Figure 5. Comparing the spatial patterns of return levels (Figure 5) with those of the parameters

(Figure 3), it is obvious that the trend of the location parameter μ_1 reflects the major features of that of 2-year return level. This is because when $p = 0.63$, z_p is governed mainly by μ in Equation 3 and τ is close to 2 years via Equation 2. As such, the trend of return level is mainly determined by the location parameter (μ_1) for the 2-year return level. The trends of 20-year return level, however, begin to be influenced more and more by the trend of scale parameter (σ_1).

According to Table 2, the trends of the two non-stationary parameters (μ_1 and σ_1) have identical signs at 20 of 24 stations. As a consequence, the trends of the return levels corresponding to longer return periods are in the same direction as that of 2-year return level and their slopes become steeper (e.g. Figure 4(b)). There is also island-wide consistency where both parameters have negative trends on Oahu and Maui and positive trends on the Island of Hawaii (Table 2). This is exemplified in Figure 5. When the signs of μ_1 and σ_1 are opposite, such as Stations 2 and 6 on Oahu, and Station 17 on the Island of Hawaii, the slopes become gentle and even change sign. One of the most noteworthy cases is the Station 17, Paauilo, which is located in the northern part of the Island of Hawaii. It has a positive trend in 2-year return level (Figure 5(a)), but a negative trend in 20-year and 100-year return level (Figure 5(b) and (c)). The time series of return levels at this station is shown in Figure 4(c).

Table 3. Signs of the slopes of non-stationary GEV parameters according to the SOI values. Field significance is reached only for the Island of Hawaii.

Station ID	1-day	
	GEV μ_1	GEV σ_1
1	+	+
2	+	+
3	+	+
4	+	−
5	+ (*)	+ (*)
6	+	+
7	+	+
8	+	+
9	+	+
10	+	+
11	+	+
12	+	+
13	+	+
14	+	−
15	+ (*)	+ (*)
16	+	+
17	+ (*)	+ (*)
18	+ (*)	− (*)
19	+ (*)	+ (*)
20	+ (*)	+ (*)
21	+ (*)	+ (*)
22	+ (*)	+ (*)
23	+	−
24	+ (*)	+ (*)

4.3. Relationship between precipitation extremes and ENSO

As mentioned in Section 3.4, another usage of the non-stationary GEV distribution is to analyze the relationship between precipitation extremes and time-variant indicators. Chu and Chen (2005) showed that Hawaiian winter precipitation is sensitive to the ENSO phenomenon, which operates on an interannual time scale. More recently, Chu *et al.* (2010) suggested there are similar relationships between climate change indices of precipitation extremes and ENSO. As described in Section 1, these indices are different from what are applied in this study. Moreover, besides examining changes in precipitation extremes solely with time, the non-stationary GEV distribution can also be used to investigate how extreme events will co-vary with an external climate forcing. Here, the relationship between extreme precipitation and SOI will be analyzed using the non-stationary GEV distribution.

The signs of the slopes of GEV parameters (μ_1 and σ_1) according to SOI values are given in Table 3, and those that are significant at the 5% level are highlighted with stars. The positive relationship between extremes and the location parameter μ_1 is overwhelming; this means that when SOI is large and positive, which is indicative of a La Niña event, those stations listed in Table 3 tend to receive heavier precipitation. Conversely, when the SOI is large and negative (i.e. El Niño years), there are moderate extreme events. As shown in Table 3, the signs of the scale parameter σ_1 are not always in the same direction as those of the location parameter μ_1. This phenomenon, similar to those results according to time, shows the influence of the scale parameter σ_1 on the trends of 20- and 100-year return levels. That is to say, when the sign of the slope of the scale parameter is in the same direction as those of the location parameter, the relationship between extremes and SOI are enhanced for 20- and 100-year return levels. The reverse is true if these two parameters vary in an opposite manner.

The spatial patterns of the GEV parameters for 1-day maximum precipitation as co-variant with SOI values are shown in Figure 6. Out of the three major islands studied, it appears that the trends of non-stationary parameters are most clear on the Island of Hawaii. Because the Island of Hawaii is located closer to the anomalous heating center in the equatorial central Pacific, its connection to the equatorial ENSO phenomenon is perhaps stronger than more northern islands such as Oahu.

Figure 7 shows the relationship between return levels of 1-day maximum precipitation and SOI at Stations 20 (Kulani Camp) and 18 (Hilo). Again, these results are obtained after transforming the precipitation data back to the original amounts. The relationship between extremes and SOI are all significant at the 5% level at these two stations (Table 3); however, the signs of the location parameter μ_1 and the scale parameter σ_1 are in the same direction at Station 20, but opposite at Station 18. As a result, relative to the 2-year return level, the 20- and 100-year return levels strongly increase when

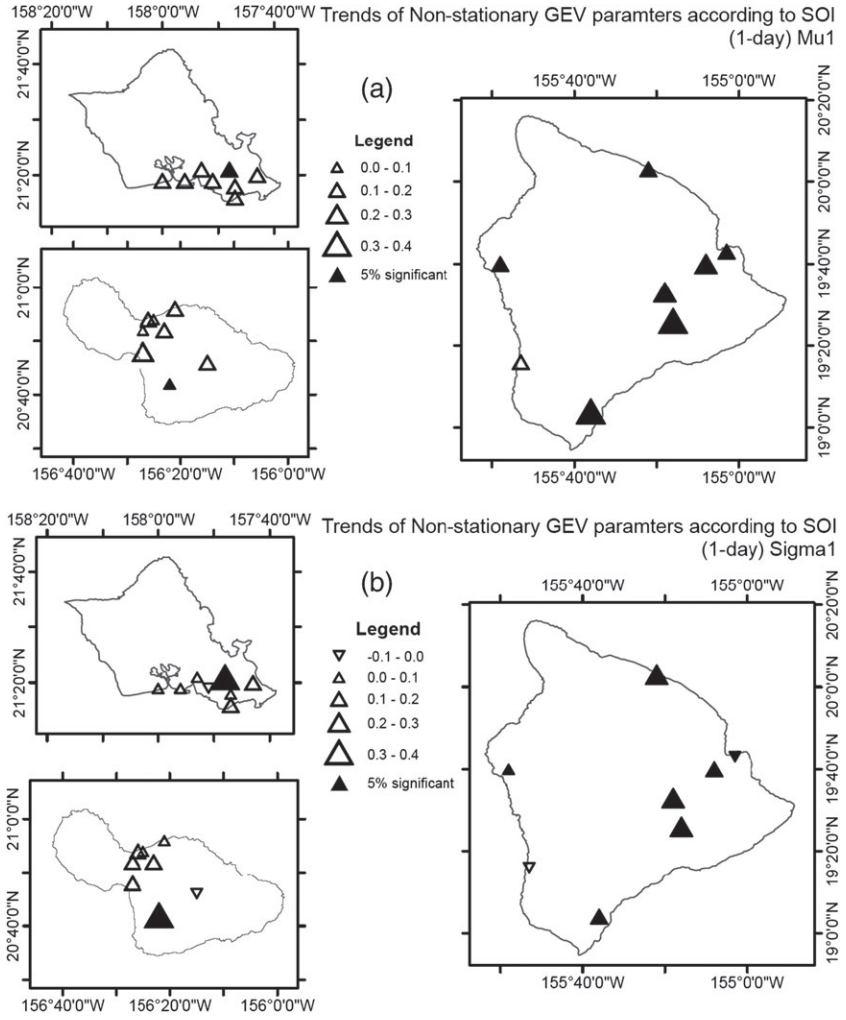

Figure 6. Spatial pattern of trends for (a) location parameter μ_1 and (b) scale parameter σ_1 for 1-day maximum precipitation according to SOI value using non-stationary GEV distribution. Triangles denote the locations of the individual stations. Upward (downward) triangles indicate positive (negative) direction of change, and their size corresponds to the magnitude of relationship. Black triangles indicate trends significant at the 5% level. Field significance is reached for the Island of Hawaii in (a) and (b).

SOI values increase at Kulani Camp. On the other hand, the increasing tendencies of the 20- and 100-year return levels are milder at Hilo International Airport than that of the 2-year return level. The dependence of precipitation extremes on the SOI is assessed through the goodness-of-fit for these two stations. By incorporating a covariate into the parameters of the GEV, the standardized variables will then have a standard Gumbel distribution (Coles, 2001, p. 110). The quantile-quantile plot (not shown) indicates that the fitted distribution corresponds well to the empirical data, with a R^2 of 99.2% for Kulani Camp and 98.5% for Hilo International Airport. Although other research has also indicated the relationship between Hawaii precipitation and Pacific Decadal Oscillation (PDO; Chu and Chen, 2005 and Chu *et al.*, 2010; Elison Timm *et al.*, 2011), the current study focused on the ENSO related variability as the most dominant climate mode in the tropical Pacific. Our preliminary analysis suggests that relationship between precipitation extremes in Hawaii and PDO is not as strong as that between precipitation extremes and SOI.

5. Conclusions

In this study, changes in annual maximum 1-day precipitation amounts at 24 stations in Oahu, Maui, and the Island of Hawaii are analyzed. First, a nonparametric Mann-Kendall test and Sen's method were applied to detect trends of precipitation extremes. The most outstanding feature is the prevalence of negative trends on Oahu and Maui and positive trends on the Island of Hawaii (Table 2). Therefore, the trend patterns in precipitation extremes are not necessarily the same across the Hawaiian Islands over the last 50 years. This is followed by a non-stationary GEV distribution fitted into the data sets and the trends of the location and scale parameters, and trends of 2-, 20, and 100-year return levels were calculated while holding the shape parameter constant. The results bear a close resemblance to the nonparametric trend-detection methods in the sense that negative trends dominate on Oahu and Maui but positive trends prevail on the Island of Hawaii. We also examine the contribution of changes in the location parameter μ_1 and scale

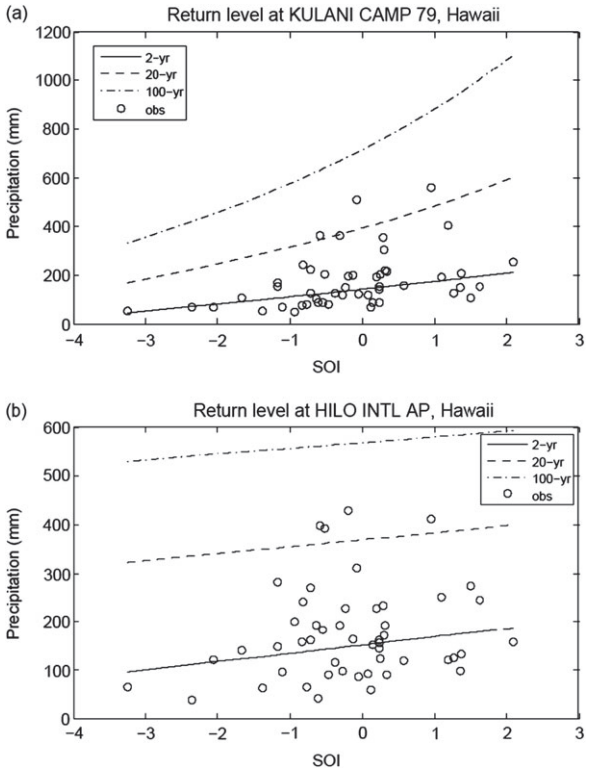

Figure 7. Relationship between return levels of 1-day maximum precipitation and SOI at (a) Kulani Camp (station 20) and (b) Hilo International Airport (station 18), Hawaii according to non-stationary GEV. The solid, dashed, and dash-dot lines represent the 2-year, 20-year, and 100-year return levels, respectively. The circles stand for observation data.

parameter σ_1 to the return levels. The former variable is more important for the 2-year return level, and the latter is more influential for the 20- and 100-year return levels.

The relationship between precipitation extremes and SOI are analyzed using a non-stationary GEV distribution. A positive association is found, which implies that there are intense extreme events during La Niña years but moderate extreme events (low precipitation extremes) during El Niño years. This phenomenon is more evident on the Island of Hawaii.

Perica *et al.* (2009) and Chu *et al.* (2009) independently used a stationary GEV model to produce the statistics of extreme precipitation values in Hawaii. For engineering design (e.g. urban drainage) and environmental regulations in Hawaii, return-period rainfall amounts are assumed to be constant at a given threshold level (e.g. 100-year return level). Because the climate is changing, the assumption of stationary precipitation climatology is questionable and needs to be reconsidered. The return-level threshold periods have changed considerably for many stations in Hawaii. As a result, a rare storm with daily precipitation of 300 mm, which is regarded as a 20-year return period in 1960, has become a rather common storm event with a return period of 3–5-year in 2009 on the Island of Hawaii. Put in a different way, heavy rainfall events have become more frequent over the last 50 years on the Island of Hawaii, and this change has repercussions on property, human life, transportation, health, and ecological systems. Based on a non-stationary GEV model, our study provides new information concerning changes in precipitation extremes and recurrence times.

Acknowledgements

We appreciate constructive comments from Rick Katz and Oliver Elison Timm for this study. Andre Marquez helped with the analysis of comparing the return-level intensity for the complete and incomplete data sets, also the analysis of POT series. Partial support for this study came from the Hawaii State Climate Office, which is funded by the School of Ocean and Earth Science and Technology, University of Hawaii-Manoa.

References

Alexander LV, Zhang X, Peterson TC, Caesar J, Gleason B, Klein Tank AMG, Haylock M, Collins D, Trewin B, Rahimzadeh F, Tagipour A, Rupa Kumar K, Revadekar J, Griffiths G, Vincent L, Stephenson DB, Burn J, Aguilar E, Brunet M, Taylor M, New M, Zhai P, Rusticucci M, Vazquez-Aguirre JL. 2006. Global observed changes in daily climate extremes of temperature and precipitation. *J. Geophys. Res.* **111**: D05109, DOI: 10.1029/2005JD006290.

Chu P-S, Chen H. 2005. Interannual and interdecadal rainfall variations in the Hawaiian Islands. *J. Clim.* **18**: 4796–4813.

Chu P-S, Wang J. 1997. Recent climate change in the tropical western Pacific and Indian Ocean regions as detected by outgoing longwave radiation records. *J. Clim.* **10**: 636–646.

Chu P-S, Nash AJ, Porter F-Y. 1993. Diagnostic studies of two contrasting rainfall episodes in Hawaii: dry 1981 and wet 1982. *J. Clim.* **6**: 1457–1462.

Chu P-S, Zhao X, Ruan Y, Grubbs M. 2009. Extreme rainfall events in the Hawaiian Islands. *J. Appl. Meteorol. Climatol.* **48**: 502–516.

Chu P-S, Chen YR, Schroeder TA. 2010. Changes in precipitation extremes in the Hawaiian Islands in a warming climate. *J. Clim.* **23**: 4881–4900.

Chu P-S, Chen DJ, Lin P-L. 2014. Trends in precipitation extremes during the typhoon season in Taiwan over the last 60 years. *Atmos. Sci. Lett.* **15**: 37–43.

Coles S. 2001. *An Introduction to Statistical Modeling of Extreme Values*. Springer-Verlag: London.

Douglas EM, Vogel RM, Kroll CN. 2000. Trends in floods and low flows in the United States: impact of spatial correlation. *J. Hydrol.* **240**: 90–105.

Elison Timm O, Diaz HF, Giambelluca TW, Takahashi M. 2011. Projection of changes in the frequency of heavy rain events over Hawaii based on leading Pacific climate modes. *J. Geophys. Res.* **116**: D04109, DOI: 10.1029/2010JD01492.

Frich P, Alexander LV, Della-Maria P, Gleason B, Haylock M, Klein Tank AMG, Peterson T. 2002. Observed coherent changes in climatic extremes during the second half of the twentieth century. *Clim. Res.* **19**: 193–212.

García JA, Gallego MC, Serrano A, Vaquero JM. 2007. Trends in block-seasonal extreme rainfall over the Iberian Peninsula in the second half of the twentieth century. *J. Clim.* **20**: 113–130.

Giambelluca TW, Schroeder TA. 1998. The physical environment: climate. In *Atlas of Hawaii*, 3rd edn, Juvik SP, Juvik JO (eds). University of Hawaii Press: Honolulu, HI; 49–59.

Griffiths ML, Bradley RS. 2007. Variations of twentieth-century temperature and precipitation extreme indicators in the northeast United States. *J. Clim.* **20**: 5401–5417.

Groisman PY, Knight RW, Karl TR, Easterling DE, Sun B, Lawrimore JH. 2004. Contemporary changes of the hydrological cycle over the contiguous United States: trends derived from in situ observations. *J. Hydrometeorol.* **5**: 64–85.

Hosking JRM, Wallis JR, Wood EF. 1985. Estimation of the generalized extreme-value distribution by the method probability-weighted moments. *Technometrics* **27**: 251–261.

Katz RW, Parlange MB, Naveau P. 2002. Statistics of extremes in hydrology. *Adv. Water Resour.* **25**: 1287–1304.
Kendall MG. 1970. *Rank Correlation Methods*, 2nd edn. Hafner: New York, NY.
Kharin VV, Zwiers FW. 2005. Estimating extremes in transient climate change simulations. *J. Clim.* **18**: 1156–1173.
Kodama K, Barnes GM. 1997. Heavy rain events over the South-Facing slopes of Hawaii: attendant conditions. *Weather Forecast.* **12**: 347–367.
Livezey RE, Chen WY. 1983. Statistical field significance and its determination by Monte-Carlo techniques. *Mon. Weather Rev.* **111**: 46–59.
Lyman RE, Schroeder TA, Barnes GM. 2005. The heavy rain event of 29 October 2000 in Hana, Maui. *Weather Forecast.* **20**: 397–414.
Mann HB. 1945. Nonparametric tests against trend. *Econometrica* **13**: 245–259.
Norton CW, Chu P-S, Schroeder TA. 2011. Projecting changes in future heavy rainfall events for Oahu, Hawaii: a statistical downscaling approach. *J. Geophys. Res.* **116**: D17110, DOI: 10.1029/2011JD015641.
Perica S, Martin D, Lin B, Parzybok T, Riley D, Yekta M, Hiner L, Chen L-C, Brewer D, Yan F, Maitaria K, Trypaluk C, Bonnin GM. 2009. *Precipitation-Frequency Atlas of the United States Vol. 5, Selected Pacific islands, NOAA Atlas 14*. U. S. Department of Commerce, National Oceanic and Atmospheric Administration, National Weather Service: Silver Spring, MD.
Pettitt AN. 1979. A nonparametric approach to the change point problem. *Appl. Stat.* **28**: 126–135.
Schroeder TA. 1977. Meteorological analysis of an Oahu Flood. *Mon. Weather Rev.* **105**: 458–468.
Sen PK. 1968. Estimates of the regression coefficient based on Kendall's tau. *J. Am. Stat. Assoc.* **63**: 1379–1389.
Wilks DS. 2011. Statistical Methods in the Atmospheric Sciences, 3rd edn. Academic Press: San Diego, CA.
Zolina O, Simmer C, Kapala A, Gulev S. 2005. On the robustness of the estimates of centenal-scale variability in heavy precipitation from station data over Europe. *Geophys. Res. Lett.* **32**: L14707.

